



DOI: 10.18720/MCE.94.12

Micromechanical characteristics of high-performance concrete subjected to modifications of composition and homogenization

P. Bily*, J. Fladr, R. Chylik, V. Hrbek, L. Vrablik
 Czech Technical University, Prague, Czech Republic
 * E-mail: petr.bily@fsv.cvut.cz

Keywords: high-performance concrete, supplementary cementitious materials, interfacial transition zone, nanoindentation, mechanical pro

Abstract. The paper deals with the effect of various modifications of composition and homogenization procedure on micromechanical characteristics of high-performance concrete (HPC) containing supplementary cementitious materials (SCMs), namely silica fume, fly ash and metakaolin. The main motivation was to characterize the changes of microstructure induced by the type and amount of SCMs, by the time and order of mixing of components and by coarse aggregate washing. The effects of the changes of microstructure on macroscopic mechanical features of the material were also studied. Indentation moduli of particular phases of the material were measured by nanoindentation. Interfacial transition zone (ITZ) thickness was primarily measured by nanoindentation. An alternative method of ITZ thickness determination based on variations in chemical composition was tested for a selected sample with encouraging result. Compressive strength and bulk elastic modulus of concrete were determined by standard loading tests. The results showed that SCMs generally decrease the thickness of ITZ, but no direct relation to compressive strength of concrete was found for mixtures with variable SCMs content. In case of mixtures with optimized SCMs content prepared by different homogenization procedures or with the use of aggregate washing, qualitative dependence between ITZ thickness and compressive strength was found. Aggregate washing proved to be useful for improving both microscopic and macroscopic properties, having positive effect on ITZ thickness, compressive strength, bulk elastic modulus and indentation moduli of particular phases.

1. Introduction

Interfacial transition zone (ITZ) and its properties are one of the most important, but at the same time the least understood phenomena influencing mechanical properties of concrete. ITZ is a thin transitional layer between aggregate grains and cement paste. It is a weak link in the structure of a cementitious composite, where the first microcracks originate and begin to develop into macrocracks. A typical thickness of ITZ in normal strength concrete reaches 30 – 100 μm [1–3], while in high-performance composites, lower values ranging between 10–30 μm are reported [4–7]. Some research works point out a strong relationship between the characteristics of ITZ (mainly its thickness and mechanical properties) and macroscopic properties of concrete, such as compressive and tensile strength, elastic modulus or resistance to deicing chemicals [8–10].

The origin and creation of ITZ is attributed mainly to the wall effect. The phenomenon leading to accumulation of batch water on the surface of aggregate grains and local increase of water-to-binder ratio (w/b) was described by Escadeillas and Maso [11]. The local increase of w/b leads to increased porosity and decreased strength of ITZ. Another important factor is the filtration effect described by Lagerblad and Kjellsen [12]. When more aggregate grains are located close to each other, cement particles get filtrated as fresh cement paste passes through the narrow gap between the grains during concreting. As a result, an area of cement matrix with lower density and higher porosity is created. Microbleeding and syneresis also contribute to ITZ formation. Microbleeding is defined as flocking of microscopic droplets of bleeding water around larger aggregate grains in the course of concrete mixing [13]. During syneresis, cement matrix shrinks and the water is released from the structure of cement gel, leading to the separation of the water rich in cement particles from the solid components of the matrix [14].

Bily, P., Fladr, J., Chylik, R., Hrbek, V., Vrablik, L. Micromechanical characteristics of high-performance concrete subjected to modifications of composition and homogenization. Magazine of Civil Engineering. 2020. 94(2). Pp. 145–157. DOI: 10.18720/MCE.94.12



This work is licensed under a [CC BY-NC 4.0](https://creativecommons.org/licenses/by-nc/4.0/)

The works cited above identified several ways of efficient reduction of ITZ thickness. The main ones are minimization of w/b, use of superplasticizers and the use of supplementary cementitious materials (SCMs). Other influencing factors are humidity, porosity, absorbability and granulometry of aggregate, cement type, time of homogenization and compaction of the mixture and cleanness of aggregate surface. In case of high-performance concrete (HPC), Portland cement is used, w/b is already minimized to maximum possible extent, superplasticizers are used in high dosages, the aggregates with the best available properties are exploited. Therefore, it makes sense to study the remaining factors – the use of SCMs, technological process of concrete production and cleanness of aggregate surface.

SCMs are nowadays often used to improve various properties of concrete – physical and mechanical characteristics [15–18] or consistence [19]. Fediuk et al. proved that they can also increase the efficiency of grinding of cement [20] or shock resistance of concrete [21].

The positive influence of SCMs on ITZ thickness was observed by Rossignolo [22] who reported that replacing 10 % cement weight by silica fume led to the reduction of ITZ thickness by 36 % compared to reference concrete. When he modified concrete by SBR latex admixture in the dosage of 5 % and 10 % of cement weight, ITZ thickness was reduced by 27 % and 36 % respectively. The best results were obtained by combined use of silica fume (10 % cem. wt.) and SBR latex (10 % cem. wt.) when ITZ thickness was reduced by 64 %.

Duan et al. [23] investigated the effect of slag, metakaolin and silica fume on thickness and microhardness of ITZ and macroscopic compressive strength of concrete. The measurements were performed at the ages of 3, 7, 28 and 180 days for mixtures with 10 % cement weight replacement. The tendency to decrease ITZ thickness in time was evident for all the mixtures including the reference one, but it was more pronounced in the mixtures containing SCMs. In case of reference concrete, ITZ thickness was reduced from 80 μm at 3 days to 60 μm at 180 days. ITZ in concrete containing slag was reduced from 60 μm to 50 μm and in concrete containing silica fume or metakaolin the reduction from 50 μm to 40 μm was observed during the same period. The SCMs also positively influenced the microhardness of ITZ. Microhardness of ITZ constituted 79 % of microhardness of bulk cement paste in case of reference concrete, 83 % in case of concrete containing metakaolin or slag and 86 % in case of concrete containing silica fume. It was also proved that there is a direct linear dependence between microhardness of cement paste and macroscopic compressive strength of concrete.

Nilli and Ehsani [24] focused on the effect of nanosilica and silica fume on ITZ and strength development. Among other results, it was shown that replacing 5 % or 7.5 % cement weight by silica fume increased concrete compressive strength by approximately 10 %.

When studying self-compacting concretes, several researchers [25–27] confirmed that missing vibrations during concrete placement lead to elimination of vibration-induced segregation and microbleeding. The amount of water accumulated on the surface of aggregate grains was also reduced, leading to mitigation of wall effect, reducing porosity of ITZ and permeability of concrete. Yoo et al. [28] proved that the concrete placement method influences the first cracking strength and corresponding toughness of HPC.

Hiremath and Yaragal [29] experimented with the sequence of addition of compounds (microsilica before/after water, aggregate before/after water, water added in two or three steps) into HPC mixture containing 20 % silica fume (20 % cem. wt.). The highest compressive strength of 128 MPa was reached when aggregate was added to wet mortar; the standard mixing procedure (adding water to dry mix of all constituents) led to 105 MPa, i.e. 20 % less.

While some fine fillers are used to optimize the grading curve of aggregate, increase packing density of concrete and increase its compressive strength, the presence of another types of fine particles in concrete is undesirable. These include clay and other fine components (smaller than 0.125 mm) that are formed during the extraction of basalt aggregates and that are trapped on the surface of coarse aggregate grains. These particles can weaken the link between the aggregate and cement matrix and deteriorate mechanical properties of concrete [30, 31]. By increasing the amount of water bonded on the surface of aggregate grains, they locally increase the w/b in the vicinity of these grains. Cepuritis and Mørtzell [32] experimentally verified that the use of washed aggregate improves workability of concrete. However, no studies dealing with the effect of cleanness of aggregate surface (aggregate washing) on mechanical properties of concrete were found.

The paper deals with the effect of various modifications of composition and homogenization procedure on micromechanical characteristics of high-performance concrete (HPC) containing supplementary cementitious materials (SCMs). Silica fume, fly ash and metakaolin were used as partial replacement of cement. The studied modifications consisted in the type and amount of SCMs, the time and order of mixing of components and in coarse aggregate washing. The measured micromechanical characteristics were indentation moduli of individual phases of the material and thickness of interfacial transition zone (ITZ) determined by nanoindentation. Relations between the changes on the microscale and main macroscopic mechanical properties (compressive strength and bulk elastic modulus) were studied.

In their previous study [33], the authors of this paper dealt with the effect of SCMs and homogenization procedure on macroscopic mechanical properties of HPC. A large database of results was obtained, showing the relations between the modifications in composition and homogenization of HPC and a variety of macroscopic mechanical properties of the material. The main motivation of the experimental program presented in this paper was to characterize the changes of properties of the same materials on microscopic level and to study the relations between the microscopic and macroscopic mechanical features of the material. In addition to that, the effect of cleanness of aggregate surface (aggregate washing) was observed in order to evaluate the hypothesis that with cleaner coarse aggregate grains, both microscopic and macroscopic mechanical properties will be improved. As the literature review has shown, there is a very limited number of studies dealing with these topics. The authors of this paper have previously published small sets of data in two preliminary reports [34–35]. This paper provides a systematic and comprehensive study of a wide set of materials and their properties.

In accordance with the previous research study of the authors of this paper [33] and pursuing the studies of other authors cited above, the aims and tasks of the presented experimental program were:

- To determine the effect of the type and amount of SCMs on micromechanical properties of HPC.
- To determine the effect of changes in homogenization procedure, namely various mixing times and sequence of addition of components, on micromechanical properties of HPC.
- To determine the effect of aggregate washing on micromechanical properties of HPC.
- To compare the changes of micromechanical characteristics with the changes of the main macromechanical properties – compressive strength and bulk elastic modulus.

2. Methods

2.1. Investigated materials

In agreement with the preceding study of macroscopic properties [33], ten mixtures described in Table 1 were tested. REF is the reference mixture with no SCMs; MIC are the mixtures containing microsilica; POP are mixtures containing fly ash; and MET are mixtures containing metakaolin. The number 10, 20 or 30 designates the percentage of cement weight replaced by SCMs. The details regarding mixture design, chemical composition and particle size distribution of cementitious materials can be found in [33] and [36].

Table 1. Composition of the mixtures (values in $[\text{kg}/\text{m}^3]$; water-to binder ratio w/b is dimensionless).

Compound	Specification	REF	MIC10	MIC20	MIC30	POP10	POP20	POP30	MET10	MET20	MET30
cement	CEM I 42,5 R	800	720	640	560	720	640	560	720	640	560
admixture	microsilica	0	80	160	240	0	0	0	0	0	0
	fly ash	0	0	0	0	80	160	240	0	0	0
	metakaolin	0	0	0	0	0	0	0	80	160	240
water	-	210	231	252	273	197	185	172	210	210	210
w/b	-	0.26	0.26	0.26	0.26	0.26	0.26	0.26	0.26	0.26	0.26
aggregate (basalt)	8-16 mm	320	320	320	320	320	320	320	320	320	320
	4-8 mm	390	390	390	390	390	390	390	390	390	390
	0-4 mm	730	730	730	730	730	730	730	730	730	730
Superplasticizer	Polycarboxylate	25.0	33.0	33.0	33.0	34.0	32.0	30.0	30.0	30.0	30.0

For the remaining part of the experimental program, just the mixtures with optimal content of SCM from the point of view of macroscopic mechanical properties [33] were selected. Therefore, the effect of homogenization procedure and aggregate washing was measured only for REF, MIC20, POP30 and MET20.

To study the effect of homogenization procedure, four variants of the mixtures were prepared using a pan laboratory mixer with centre shaft (pan fixed, scraper moving) and nominal volume of 80 litres at the speed of 30 rpm. Details are given in Table 2.

- P1: Standard procedure used in the rest of the experimental program
- P2: SCM was added before cement.
- P3: SCM was added as the last component.
- P4: Mixing time of SCM was increased from 180 s to 300 s.

Table 2. Plans of mixing procedures P1 – P4 (the lengths of the steps are given in seconds).

Step no.	P1	P2	P3	P4
1		Aggregate 8/16+4/8 (20)		
2		Aggregate 0/4 (20)		
2	Cement (20)	SCM (180)	Cement (20)	Cement (20)
3	SCM (180)	Cement (20)	Water+SPF (60)	SCM (300)
4	Water+SPF (60)	Water+SPF (60)	SCM (180)	Water+SPF (60)

The effect of aggregate washing was studied by comparing the properties of two types of mixtures. In case of “U” type (unwashed) mixtures, the aggregate was used as received from the quarry; no special processing was carried out. In case of “W” type (washed) mixtures, the coarse fractions of the aggregate (4–8 mm and 8–16 mm) were washed and dried before mixing. To wash the aggregate, it was immersed for 30 seconds into water in running laboratory mixer, then filtered, dried in laboratory dryer and kept in laboratory conditions for 7 days to reach the same natural humidity as the unprocessed aggregate. The efficiency of the applied method of aggregate washing was confirmed by grading test that showed that the content of fine particles smaller than 0.125 mm was lowered by 94 % in 8–16 mm fraction and by 96 % in 4–8 mm fraction.

2.2. Nanoindentation

Micromechanical characteristics of individual phases of the material were obtained by displacement driven grid indentation using Ti 700 series nanoindenter (Hysitron Inc.). The method is based on injection of the tip of the probe into the material. The dependency of the applied force on the depth of penetration is measured. The mechanical properties are then computed using Oliver-Pharr theory [37] from the unloading part of the loading curve. The results of the measurements are microhardness (H) and effective elastic indentation modulus (E_r).

The samples for nanoindentation and microscopic analysis were extracted from macroscopic samples (100 mm cubes) stored in water in laboratory conditions (20–22 °C) for 28 days (identical to samples for macroscopic tests). The extracted samples were treated using grinding and polishing media. Due to mechanical heterogeneity of the material, a method reducing selective abrasivity was applied. This allowed to obtain specimens having both adequate surface roughness and compact ITZ between aggregate and matrix.

Particular indents were driven by loading function with prescribed maximum penetration depth of 150 nm. The loading took 5 seconds. The maximum force was held for 60 seconds which allowed to significantly reduce the effect of creep and viscoelasticity of the material [37]. To obtain statistically relevant set of data regarding indentation moduli of particular material phases and to locate the position of interfacial transition zone (ITZ), a grid of 21×21 indents with spacing of 10 μm was applied on all the samples. Six rows of 100 indents (spacing of 1 μm) were then performed on each ITZ location to determine the thickness of ITZ based on the measured distribution of indentation modulus along the row of indents.

Indentation modulus was derived from spectral deconvolution of measured data (normalized histograms of indentation results). The application of this method is limited by two conditions – identical area of each indent and significantly different mechanical properties of particular phases [38]. The first condition is fulfilled by applying the displacement driven loading function. The second condition is generally not fulfilled considering very similar micromechanical properties of clinker and basalt aggregate ($E_r > 100$ GPa). This problem was solved by dividing the measurements in two levels: the matrix without the aggregate and ITZ between the matrix and the aggregate. The deconvolution procedure was then applied independently on both levels and the final results were obtained by their synthesis.

Contrary to static deconvolution, spectral deconvolution takes into account mutual interactions of phases such as the interaction between matrix and clinker (soft and hard phase). The effective indentation modulus (E_r) was determined with maximum allowed deviation of 2.5 % from experimental measurements considering Gaussian distribution of probability of results.

2.3. Scanning electron microscopy and image analysis

To investigate the phase composition of selected samples, scanning electron microscopy (SEM) in backscattered electron mode (BSE) was performed using microscope Mira II LMU equipped with electron probe microanalyzer (EPMA) from Tescan corp. (Czech Republic). After polishing, 20 nm thick layer of carbon was deposited on the surface of samples to increase electric conductivity. Since grayscale intensity in obtained BSE image depends on atomic mass [39], individual phases could be identified by image analysis using an in-house software PyPAIS [40] based on intensity and entropy thresholding.

An alternative method of assigning ITZ thickness with the use of SEM and energy-dispersive X-ray detector (EDX) based on the work of Kjellsen et al. [41] was examined for one selected sample. EDX probe from Bruker corp. (Germany) was used. In the points along a line, identification of elements and quantification

of each element's concentration was carried out. According to [41], ITZ can be identified based on the ratio of Ca/Si content in hydrated material. Lower values of Ca/Si ratio indicate the presence of ITZ. The motivation for this experiment was the fact that nanoindentation measurements of ITZ thickness are very time consuming in terms of both operator time and computer time required for data processing. The alternative method provides the results relatively quickly.

2.4. Macromechanical characteristics

Macromechanical characteristics were tested according to valid European standards [42–44]. More details regarding the methods as well as complete results and their discussion can be found in [33].

3. Results and Discussion

3.1. The effect of SCM type and amount

Microstructure of the studied HPC samples was influenced by the type and amount of SCMs in many aspects.

The indentation modulus of ITZ (Table 3) was decreased by the addition of metakaolin by approximately 10 %, while the effect of fly ash and silica fume was ambiguous. Relatively strong correlation (correlation coefficient $R = 0.7$) between the change of bulk elastic modulus (E_c) and indentation modulus of ITZ induced by the addition of SCMs was found, see figure 1.

The indentation modulus of LD CSH (low-density calcium-silicate-hydrates) and HD CSH (high-density calcium-silicate-hydrates) was increased by SCMs in all instances and the increase was directly dependent on cement replacement level (Table 3). Fly ash and metakaolin increased the modulus of HD CSH by approximately 20 %; the other changes were less significant. The increase can be explained by the fact that the pozzolanic materials contain large amount of reactive silicon dioxide (SiO_2) that reacts with portlandite ($\text{Ca}(\text{OH})_2$) to form the calcium-silicate-hydrates (CSH) [45]. However, the bulk elastic modulus of all the mixtures was lower than the one of the reference mixture, the reduction reaching up to 20 % for silica fume and metakaolin mixtures and 5–10 % for fly ash containing mixtures.

Volumetric fractions of particular phases were determined for this set of samples (Table 4). In most cases, the amount of HD CSH was lower and the amount of LD CSH was higher in mixtures containing SCMs than in the reference mixture. This partially explains the reduction of bulk elastic modulus.

The indentation modulus of Portlandite (Table 3) was significantly decreased by the addition of silica fume. Fly ash and metakaolin had slightly increasing effect with no clear dependence on the replacement level. No clear relation between SCMs and indentation modulus of clinker was observed. There was no correlation between the bulk elastic modulus and indentation moduli of phases other than ITZ, see Figure 1.

The measured ITZ thickness of all the samples (Table 2) was between 8–23 μm , which coincides with the results obtained by other authors studying high-performance concrete; thickness between 10 and 30 μm was reported [4–7]. Figure 2 shows that SCMs reduced the thickness of ITZ in almost all instances (except MET30), sometimes more than twofold. This is in accordance with results of Rossignolo [22] cited in section 1.2. However, contrary to [24], no clear dependence between ITZ thickness and macroscopic compressive strength of mixtures with varying SCM content was found. In some cases (MIC20, MIC30, MET10), ITZ thickness was significantly reduced, but the compressive strength was decreased at the same time; in another cases, even a small reduction of ITZ thickness lead to noticeable increase of compressive strength (POP20, POP30).

Table 3. Mean values and standard deviations of the indentation moduli E_r [GPa] of individual phases and mean thickness of ITZ [μm] – mixtures with different content of SCMs.

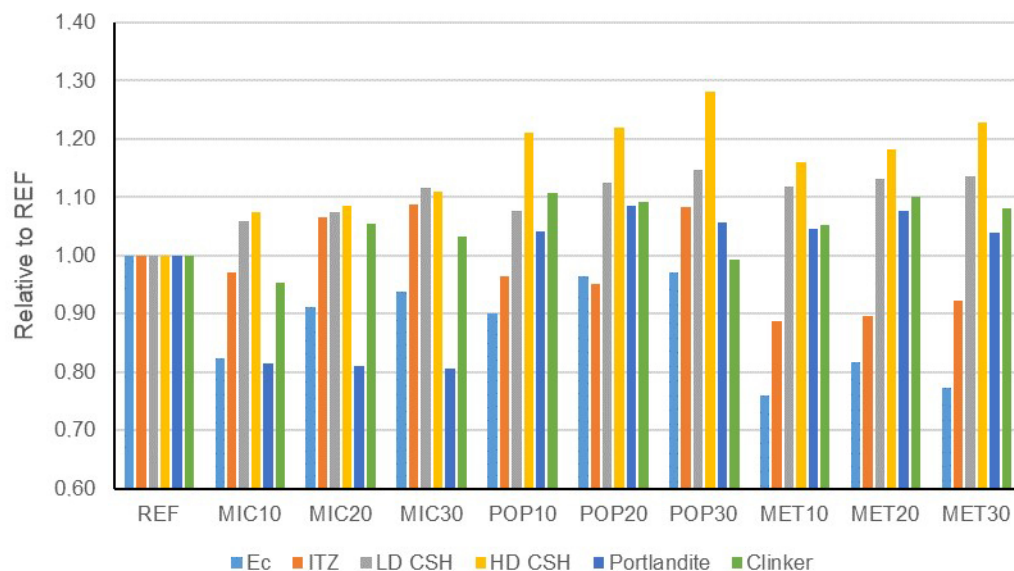
Mixture	ITZ	LD CSH	HD CSH	Portlandite	Clinker	ITZ thickness
REF	17.34±2.38	31.08±4.65	45.07±2.47	81.60±10.36	128.36±14.99	21.3
MIC10	16.82±2.18	32.91±4.16	48.43±5.78	66.55±8.50	122.28±8.50	16.1
MIC20	18.47±2.41	33.37±2.92	48.94±4.24	66.12±11.74	135.49±11.74	10.2
MIC30	18.87±3.91	34.70±3.17	49.98±3.48	65.82±6.51	132.65±6.51	8.2
POP10	16.74±2.42	33.45±5.89	54.54±7.63	84.92±14.07	142.13±13.34	16.9
POP20	16.48±2.12	34.95±5.36	54.99±6.38	88.63±13.16	140.22±12.42	13.8
POP30	18.80±4.40	35.62±5.87	57.72±6.40	86.17±7.59	127.57±16.85	14.9
MET10	15.38±1.98	34.73±4.82	52.32±8.56	85.36±12.06	135.12±18.01	12.1
MET20	15.54±3.24	35.15±6.28	53.27±8.71	87.88±14.55	141.20±18.85	15.9
MET30	16.01±2.25	35.27±5.69	55.40±6.32	84.79±10.26	138.62±14.42	23.0

Table 4. Mean values and standard deviations of volumetric fractions for individual phases – mixtures with different content of SCMs.

Mixture	LD CSH	HD CSH	Portlandite	Clinker	Aggregate
REF	15.82±0.25	15.43±0.35	6.55±0.15	4.18±0.02	56.52±1.39
MIC10	16.09±0.42	16.61±0.44	4.07±0.06	5.43±0.16	57.45±2.44
MIC20	18.30±0.98	14.57±0.17	4.49±0.13	6.48±0.22	55.56±3.31
MIC30	19.33±0.01	13.74±0.38	5.75±0.20	6.76±0.25	56.33±2.79
POP10	19.61±0.31	15.34±0.15	5.77±0.11	6.20±0.18	57.89±2.44
POP20	12.25±0.40	13.96±0.71	8.50±0.03	2.93±0.23	60.78±1.88
POP30	13.48±0.70	13.79±0.50	8.40±0.05	2.81±0.12	59.18±1.93
MET10	18.00±0.21	12.59±0.05	4.65±0.02	6.08±0.18	59.38±1.41
MET20	18.94±0.33	12.90±0.62	3.82±0.21	5.50±0.23	61.26±0.98
MET30	18.78±0.54	12.93±0.53	3.23±0.16	4.81±0.12	60.78±1.03

Table 5. Mean values of macroscopic compressive strength and bulk elastic modulus – mixtures with different content of SCMs.

Mixture	Compressive strength [MPa]	Elastic modulus [GPa]
REF	105.9	51.3
MIC10	109.3	42.2
MIC20	101.3	46.8
MIC30	97.7	48.1
POP10	106.6	46.2
POP20	120.8	49.5
POP30	125.3	49.8
MET10	108.9	39.0
MET20	110.3	41.9
MET30	96.7	39.7

**Figure 1. Bulk elastic modulus (E_c) and indentation moduli of particular phases relative to reference mixture (REF) – mixtures with different content of SCMs.**

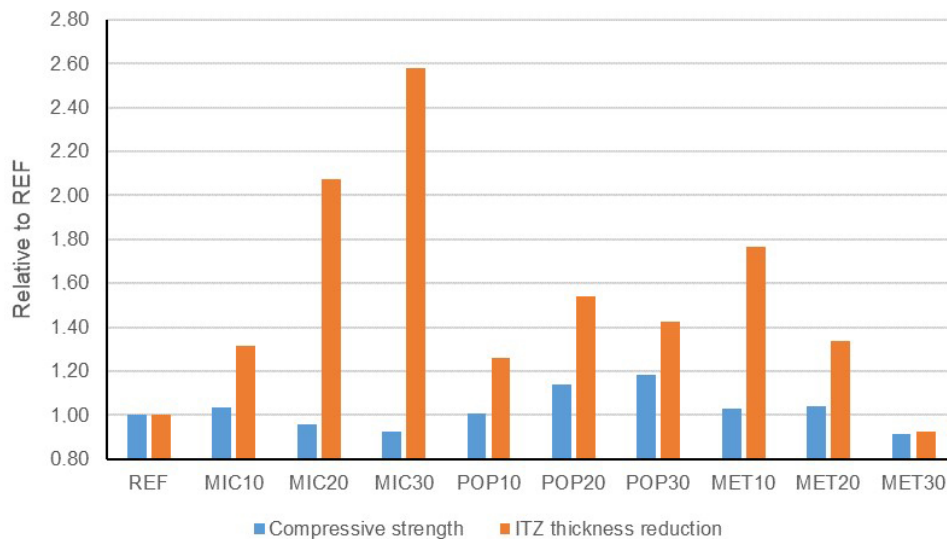


Figure 2. Compressive strength and reduction of ITZ thickness relative to reference mixture (REF) – mixtures with different content of SCMs.

For one selected sample of reference concrete (REF), an alternative method of determination of ITZ thickness was tested. The method is based on the ratio of Ca/Si content in selected points along a line. Figure 3 shows the development of Ca/Si ratio in the analysed area. When we compare the plot with the SEM photograph in figure 4, it can be concluded that points 3–7 are located inside ITZ. This indicates that the ITZ thickness is approximately 23 μm , which is in good agreement with 21.3 μm measured by nanoindentation of REF samples. Finer grid of measuring points would be required to obtain more accurate value, but the method provides very good results in relatively short time.

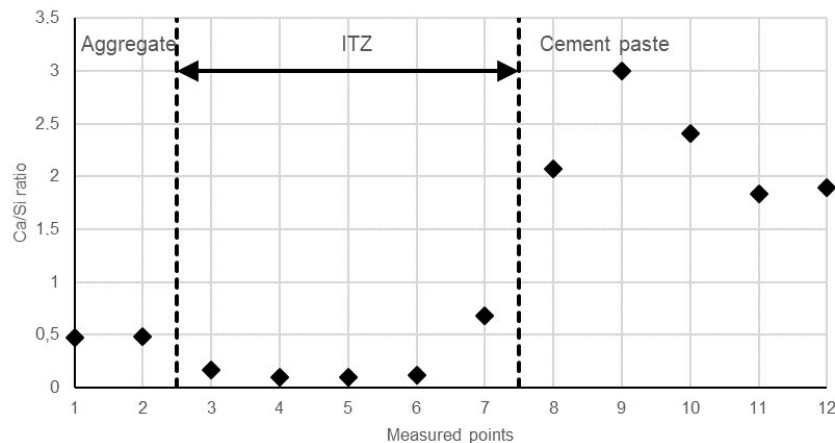


Figure 3. Ca/Si ratio along a line in a sample of reference concrete (REF).

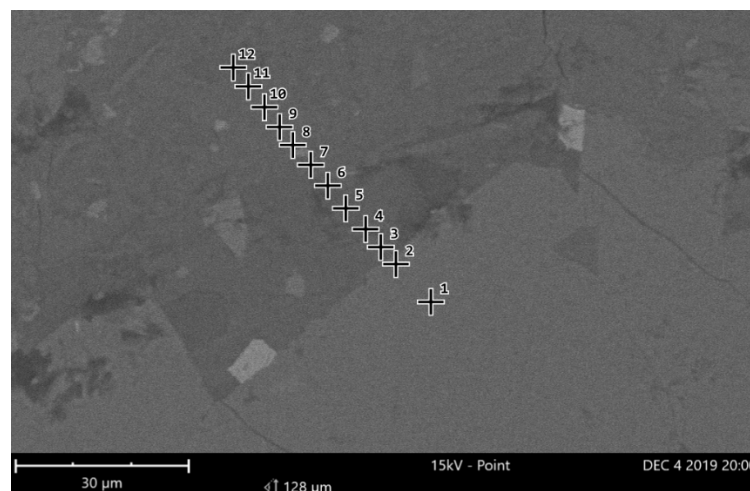


Figure 4. SEM image of the analysed area, showing the transition between an aggregate grain (points 1 and 2), ITZ and cement matrix (200x magnification).

3.2. The effect of homogenization procedure

As Tables 6 and 7 and Figure 5 demonstrate, there was no clear relation between the homogenization procedure applied and indentation moduli of particular phases or bulk elastic modulus of concrete. There was also no correlation between bulk elastic modulus and indentation moduli of any of the phases, but the common feature of mixtures with higher bulk elastic modulus (POP mixtures, MET20-2 and MET20-3) was that they had increased indentation modulus of HD CSH when compared to the reference mixture.

Relatively strong correlation ($R = 0.75$) was found between ITZ thickness and compressive strength of the material. It can be clearly seen in figure 6 that while procedure P2 always increased the ITZ thickness and mostly decreased compressive strength compared to basic procedure P1, procedure P3 lead to the reduction of ITZ thickness and increase of compressive strength. The effect of procedure P4 was ambiguous.

The fact that the homogenization procedure P3, in which the SCM was added as the last component to the wet mix, lead to improvement of the compressive strength, is in agreement with the results of Hiremath and Yaragal [29] cited in section 1.2. No other research works dealing with the effect of homogenization procedure of HPC containing SCMs that could be used for comparison of results were found.

Table 6. Mean values and standard deviations of the indentation moduli E_r [GPa] of individual phases and mean thickness of ITZ [μm] – mixtures prepared by different homogenization procedures (P1 – P4).

Mixture	ITZ	LD CSH	HD CSH	Portlandite	Clinker	ITZ thickness
REF-1	17.19±2.59	32.87±4.39	45.22±4.50	80.08±9.78	127.64±13.82	18.5
MIC20-1	18.26±2.68	33.92±4.34	48.80±4.45	69.02±9.45	134.37±10.67	18.3
MIC20-2	17.43±2.74	32.67±4.39	46.38±4.46	70.29±8.63	132.56±11.74	18.8
MIC20-3	19.81±2.82	35.2±4.42	49.28±4.45	69.57±6.08	133.62±9.56	17.3
MIC20-4	18.91±2.69	34.12±4.43	48.95±4.54	69.25±7.19	134.92±12.27	17.9
POP30-1	15.99±2.74	34.82±4.38	55.85±4.50	79.89±10.14	138.37±12.03	16.1
POP30-2	14.53±2.77	34.00±4.39	53.06±4.53	72.48±8.25	136.36±10.74	19.4
POP30-3	15.18±2.89	34.15±4.38	54.34±4.55	76.53±7.38	137.84±9.98	15.2
POP30-4	15.04±2.77	34.29±4.38	54.46±4.40	77.61±8.80	137.05±10.55	16.1
MET20-1	15.30±2.78	35.31±4.27	53.65±4.44	86.14±12.45	139.71±15.55	14.9
MET20-2	15.82±2.76	35.88±4.27	54.42±4.49	87.26±9.83	136.74±12.38	15.6
MET20-3	16.37±2.70	36.45±4.37	54.91±4.40	87.85±7.36	139.68±9.55	13.7
MET20-4	15.48±2.68	35.56±4.28	54.17±4.48	85.27±8.69	138.12±10.33	18.8

Table 7. Mean values of macroscopic compressive strength and bulk elastic modulus – mixtures prepared by different homogenization procedures (P1 – P4).

Mixture	Compressive strength [MPa]	Elastic modulus [GPa]
REF-1	105.9	51.3
MIC20-1	101.3	46.8
MIC20-2	99.0	39.8
MIC20-3	113.8	41.6
MIC20-4	103.8	40.7
POP30-1	125.3	49.8
POP30-2	95.5	49.5
POP30-3	115.8	51.0
POP30-4	109.0	50.4
MET20-1	110.3	41.9
MET20-2	118.0	52.9
MET20-3	127.7	52.5
MET20-4	115.4	45.5

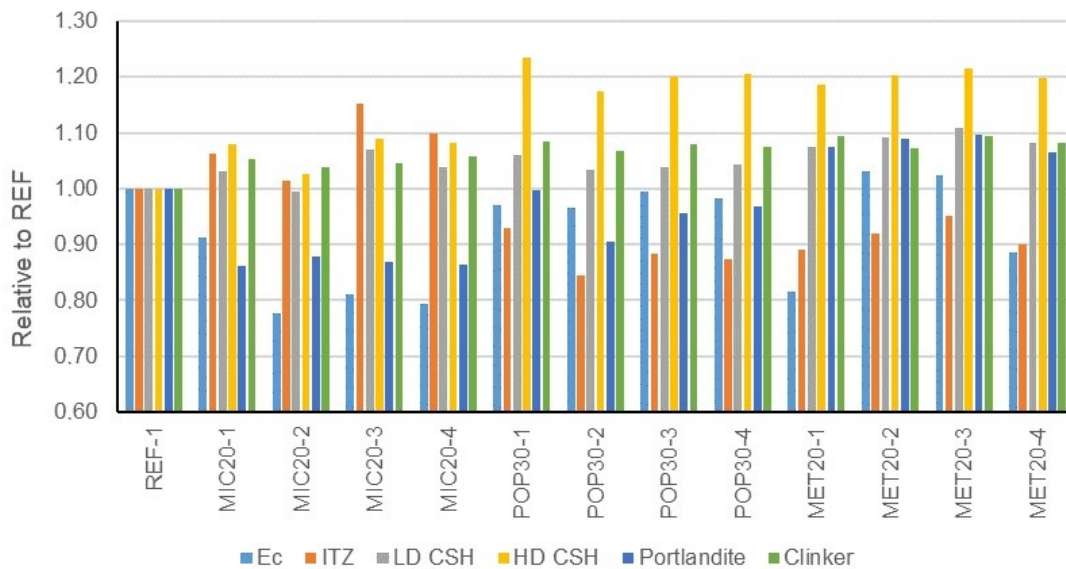


Figure 5. Bulk elastic modulus (E_c) and indentation moduli of particular phases relative to reference mixture (REF-1) – mixtures prepared by different homogenization procedures (P1 – P4).

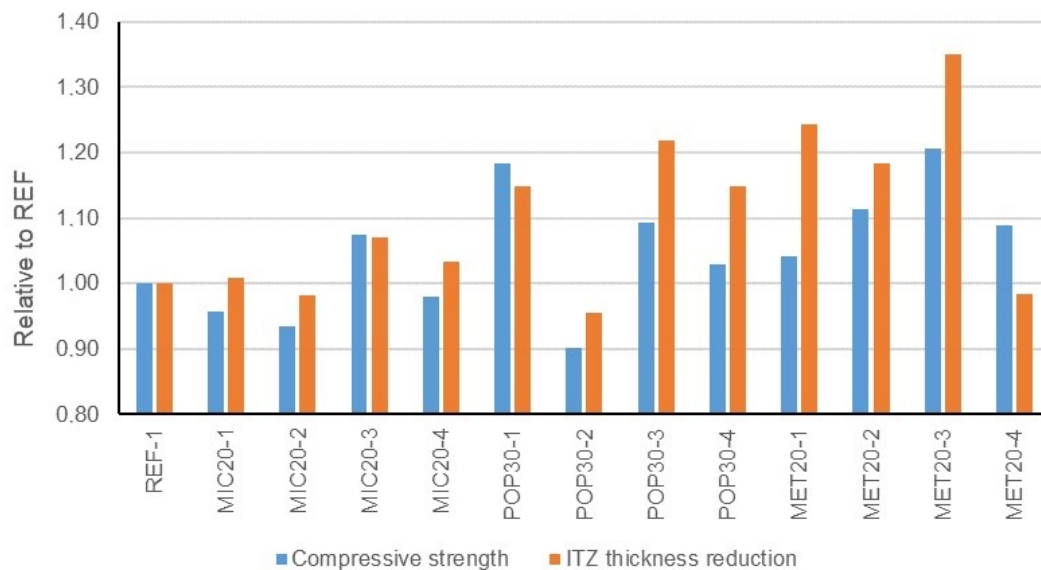


Figure 6. Compressive strength and reduction of ITZ thickness relative to reference mixture (REF-1) – mixtures prepared by different homogenization procedures (P1 – P4).

3.3. The effect of aggregate washing

The results of this part of the experimental program, which studied the effect of washing of coarse fractions of the aggregate (4–8 mm and 8–16 mm), were the clearest ones. When comparing respective mixtures with unwashed (U) and washed (W) aggregate in tables 8 and 9, it is obvious that aggregate washing always had positive effect on ITZ thickness, compressive strength and bulk elastic modulus, even though a mild one (up to 10 % in most cases). The same thing can be said about the effect on indentation moduli of particular phases (Table 8, Figure 7), but the differences are even smaller in this case (smaller than the standard deviation of the results). The positive effect of washing can be related to the fact that due to the removal of detrimental fine particles, the processed coarse aggregate had smaller relative surface area, leading to the elimination of the wall effect described in chapter 1.2.

Figure 8 depicts the relation between compressive strength and the reduction of ITZ thickness of particular mixtures. The trend was clear, when the ITZ thickness was reduced, the compressive strength was increased. However, the changes were not proportional.

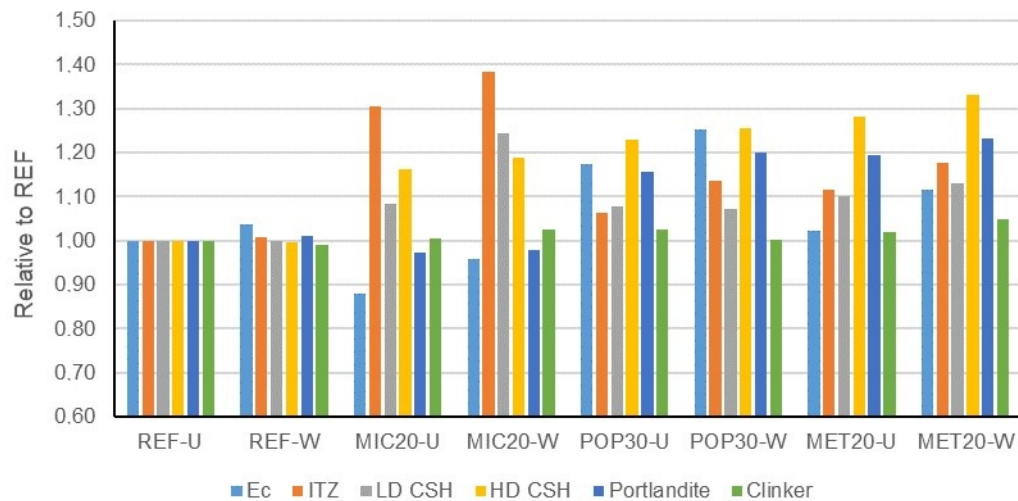
As stated in section 1.2, no studies dealing with the effect of aggregate washing on neither microscopic nor macroscopic properties of concrete were found. Therefore, the comparison of results with other authors is not possible.

Table 8. Mean values and standard deviations of the indentation moduli E_r [GPa] of individual phases and mean thickness of ITZ [μm] – mixtures with unwashed (U) and washed (W) aggregate.

Mixture	ITZ	LD CSH	HD CSH	Portlandite	Clinker	ITZ thickness
REF-U	13.55±3.59	30.96±3.63	41.03±4.04	69.77±6.91	130.55±14.71	21.7
REF-W	13.67±3.55	30.92±4.76	40.93±5.08	70.56±8.32	129.46±15.05	20.4
MIC20-U	17.69±2.46	33.54±2.68	47.73±4.14	67.87±8.58	131.35±12.46	14.1
MIC20-W	18.75±3.53	38.48±4.67	48.77±4.52	68.23±9.00	133.69±14.87	10.5
POP30-U	14.42±3.03	33.37±4.43	50.48±5.02	80.61±7.01	133.97±15.45	15.8
POP30-W	15.40±3.43	33.22±4.43	51.52±4.71	83.72±6.88	130.65±12.13	14.2
MET20-U	15.13±3.86	34.11±3.64	52.59±3.29	83.21±8.99	132.92±11.58	19.3
MET20-W	15.96±2.87	35.00±4.71	54.61±5.41	86.01±10.42	137.03±16.98	15.6

Table 9. Mean values of macroscopic compressive strength and bulk elastic modulus — mixtures with unwashed (U) and washed (W) aggregate.

Mixture	Compressive strength [MPa]	Elastic modulus [GPa]
REF-U	113.7	39.4
REF-W	118.4	40.9
MIC20-U	113.9	34.7
MIC20-W	129.1	37.7
POP30-U	125.8	46.2
POP30-W	131.0	49.3
MET20-U	114.1	40.3
MET20-W	127.3	44.0

**Figure 7. Bulk elastic modulus (E_c) and indentation moduli of particular phases relative to reference mixture (REF-U) – mixtures with unwashed (U) and washed (W) aggregate.**

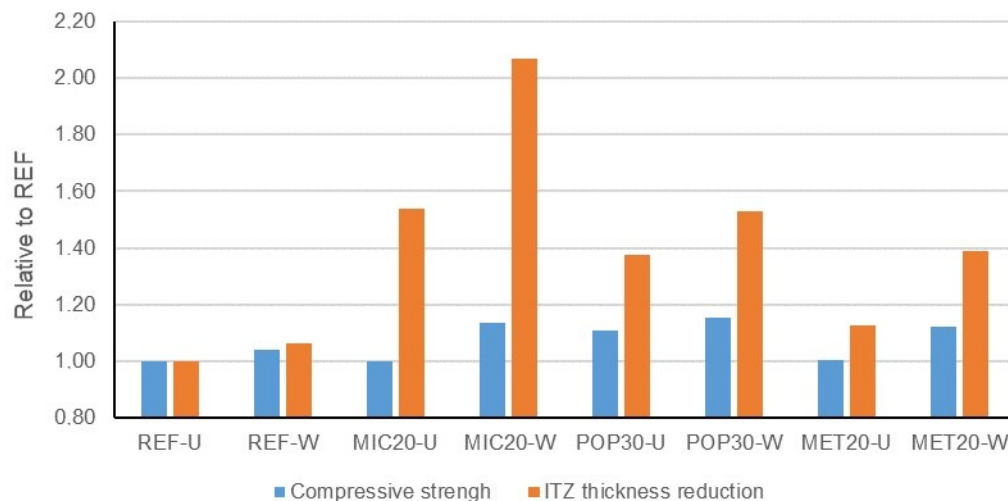


Figure 8. Compressive strength and reduction of ITZ thickness relative to reference mixture (REF-U) – mixtures with unwashed (U) and washed (W) aggregate.

4. Conclusions

The experimental program provided a comprehensive database characterizing the effects of SCM type and content, homogenization procedure and aggregate washing on micromechanical properties of HPC containing SCMs. Several qualitative trends between micromechanical and macromechanical properties of studied concrete were identified. The main conclusions are:

- SCMs increased the indentation modulus of HD CSH. There was a direct dependence on SCM content.
- When varying the SCM content, there was a direct dependence between the change of indentation modulus of ITZ and bulk elastic modulus of concrete.
- The use of SCMs generally had negative effect on bulk elastic modulus of the material. This might be related to the changes of volumetric fractions of LD CSH and HD CSH. The addition of SCMs lead to decrease of HD CSH content and increase of LD CSH content, thus increasing the share of lower-density compounds at the expense of high-density compounds.
- The previous effect was the lowest (only up to 10 %) when fly ash was used. This fact was probably connected with the increase of indentation modulus of HD CSH, which was the highest (up to 20 %) in case of fly ash containing mixtures.
- SCMs generally decreased the thickness of ITZ, in some cases more than twofold. However, there was no clear proportional dependence between ITZ thickness and compressive strength.
- The homogenization procedure of mixtures with optimized SCM content influenced the thickness of ITZ and compressive strength. Adding SCMs to the mixer before cement (P2) had generally negative effect on both, while adding SCM to wet mix (P3) proved to have positive influence. Increased mixing time (P4) had no distinctive effect.
- Aggregate washing was useful for improving both microscopic and macroscopic properties, having positive effect on ITZ thickness, compressive strength, bulk elastic modulus and indentation moduli of particular phases, even though a mild one (up to 10 % in most cases).
- The method of measuring ITZ thickness through variations of Ca/Si ratio was tested with promising results. This method will be further verified on a larger set of specimens. In case of good agreement, it could be used as a faster alternative to nanoindentation method for determination of ITZ thickness.

5. Acknowledgement

The paper was prepared thanks to the support of the Science Foundation of the Czech Republic (GAČR), project no. 17-19463S “Analysis of the relations between the microstructure and macroscopic properties of ultra-high performance concretes”.

References

1. Aitcin, P.C. High-Performance Concrete. CRC Press. London, 1998. DOI: 10.1201/9781420022636
2. Mehta, P.K., Monteiro, P.J.M. Concrete. Microstructure, Properties, and Materials, 3rd Edition. McGraw-Hill. New York, 2006. DOI: 10.1036/0071462899

3. Wang, G., Kong, Y., Sun, T., Shui, Z. Effect of water–binder ratio and fly ash on the homogeneity of concrete. *Construction and Building Materials*. 2013. 38. Pp. 1129–1134. DOI: 10.1016/j.conbuildmat.2012.09.027
4. Wu, K., Shi, H., Xu, L., Ye, G., Schutter, G.D. Microstructural characterization of ITZ in blended cement concretes and its relation to transport properties. *Cement and Concrete Research*. 2016. 79. Pp. 243–256. DOI: 10.1016/j.cemconres.2015.09.018 .
5. Branch, J., Epps, R., Kosson, D. The impact of carbonation on bulk and ITZ porosity in microconcrete materials with fly ash replacement. *Cement and Concrete Research*. 2018. 103. Pp. 170–178. DOI: 10.1016/j.cemconres.2017.10.012
6. Duan, P., Shui, Z., Chen, W., Shen, C. Efficiency of mineral admixtures in concrete: microstructure, compressive strength and stability of hydrate phases. *Applied Clay Science*. 2013. 83–84. Pp. 115–121. DOI: 10.1016/j.clay.2013.08.021
7. Gao, Y., Schutter, G.D., Ye, G., Huang, H., Tan, Z., Wu, K. Characterization of ITZ in ternary blended cementitious composites: experiment and simulation. *Construction and Building Materials*. 2013. 41. Pp. 742–750. DOI: 10.1016/j.conbuildmat.2012.12.051
8. Monteneiro, P.J.M. Microstructure of concrete and its influence on the mechanical properties. PhD dissertation. University of California, Berkeley, 1985.
9. Maso, J.C. Influence of the interfacial transition zone on composite mechanical properties. *Interfacial Transition Zone in Concrete*. E & FN SPON. London, 1996. URL: <http://drbeton.ir/wp-content/uploads/2017/03/Interfacial-Transition-Zone-in-Concrete.pdf#page=131> (date of application: 15.11.2019).
10. Kim, S.S., Qudoos, A., Jakhriani, S.H., Lee, J.B., Kim, H.G. Influence of Coarse Aggregates and Silica Fume on the Mechanical Properties, Durability, and Microstructure of Concrete. *Materials (Basel)*. 2019. 12(20). P. 3324. DOI: 10.3390/ma12203324
11. Escadeillas, G., Maso, J.C. Approach of the initial state in cement paste, mortar, and concrete. *Advances in Cementitious Materials*. 1991. 16. Pp. 169-184. URL: https://www.researchgate.net/publication/288522438_Approach_of_the_initial_state_in_cement_paste_mortar_and_concrete (date of application: 10.10.2019).
12. Lagerblad, B., Kjellsen, K.O. Normal and High Strength Concretes with Conventional Aggregates. *Engineering and Transport Properties of the Interfacial Transition Zone in Cementitious Composites*. RILEM Report 20. RILEM Publications S.A.R.L., 1999.
13. Chandra, S. *Properties of Concrete with Mineral and Chemical Admixtures. Structure and Performance of Cements*. Spon Press. London, 2002. Pp. 140–185 ISBN: 9780419233305.
14. Rooij de, M.R. *Syneresis in Cement Paste Systems*. PhD dissertation. Delft University of Technology, Delft, 2000.
15. Yoo, D.-Y., Banthia, N. Mechanical properties of ultra-high-performance fiber-reinforced concrete: A review. *Cement and Concrete Composites*. 2016. 73. Pp. 267–280. DOI: 10.1016/j.cemconcomp.2016.08.001
16. Yoo, D.-Y., Yoon, Y.-S. A Review on Structural Behavior, Design, and Application of Ultra-High-Performance Fiber-Reinforced Concrete. *International Journal of Concrete Structures and Materials*. 2016. 10(2). Pp. 125–142. DOI: 10.1007/s40069-016-0143-x
17. Fediuk, R.S., Lesovik, V.S., Mochalov, A.V., Otsokov, K.A., Lashina, I.V., Timokhin, R.A. Composite binders for concrete of protective structures. *Magazine of Civil Engineering*. 2018. 82(6), Pp. 208–218. DOI: 10.18720/MCE.82.19
18. Gaifullin, A.R., Rakhimov, R.Z., Rakhimova, N.R. The influence of clay additives in Portland cement on the compressive strength of the cement stone. *Magazine of Civil Engineering*. 2015. 59(7). Pp. 66–73. DOI: 10.5862/MCE.59.7
19. Fediuk, R.S., Lesovik, V.S., Svintsov, A.P., Gladkova, N.A., Timokhin, R.A. Self-compacting concrete using pretreated rice husk ash. *Magazine of Civil Engineering*. 2018. 79(3). Pp. 66–76. DOI: 10.18720/MCE.79.7
20. Fediuk, R., Pak, A., Kuzmin, D. Fine-Grained Concrete of Composite Binder. *IOP Conference Series: Materials Science and Engineering*. 2017. 262(1), 012025. DOI: 10.1088/1757-899X/262/1/012025
21. Fediuk, R.S., Lesovik, V.S., Liseitsev, Y.L., Timokhin, R.A., Bituyev, A.V., Zaiakhanov, M.Y., Mochalov, A.V. Composite binders for concretes with improved shock resistance. *Magazine of Civil Engineering*. 2019. 85(1). Pp. 28–38. DOI: 10.18720/MCE.85.3
22. Rossignolo, J.A. Effect of silica fume and SBR latex on the paste aggregate interfacial transition zone. *Materials Research*. 2007. 10(1). Pp. 83–86. DOI: 10.1590/S1516-14392007000100018
23. Duan, P., Shui, Z., Chen, W. and Shen, C. Effects of metakaolin, silica fume and slag on pore structure, interfacial transition zone and compressive strength of concrete. *Construction and Building Materials*. 2013. 14. Pp. 1–6. DOI: 10.1016/j.conbuildmat.2013.02.075
24. Nili, M., Ehsani, A. Investigating the effect of the cement paste and transition zone on strength development of concrete containing nanosilica and silica fume. *Materials and Design*. 2015. 75. Pp. 174–183. DOI: 10.1016/j.matdes.2015.03.024
25. Skarendahl A, Petersson Ö. Self-compacting concrete – state-of-the-art report. RILEM report 23. Cachan Cedex, France, 2001
26. Hoffmann C, Leemann A. Homogeneity of structures made with selfcompacting concrete and conventional concrete. *Proceedings of 3rd int RILEM symposium SCC*. Reykjavik, Iceland, 2003. Pp. 619–627. e-ISBN: 2912143713
27. Leemann A., Münch B., Gasser P., Holzer L. Influence of compaction on the interfacial transition zone and the permeability of concrete. *Cement and Concrete Research*. 2006. 36. Pp. 1425–1433. DOI: 10.1016/j.cemconres.2006.02.010
28. Yoo, D.-Y., Banthia, N., Zi, G., Yoon, Y.-S. Comparative biaxial flexural behavior of ultra-high-performance fiber-reinforced concrete panels using two different test and placement methods. *Journal of Testing and Evaluation*. 2017. 45(2). Pp. 624–641. DOI: 10.1520/JTE20150275
29. Hiremath, P. N., Yaragal, S. C.: Influence of mixing method, speed and duration on the fresh and hardened properties of Reactive Powder Concrete. *Construction and Building Materials* 141 (2017). Pp. 271–288. DOI: 10.1016/j.conbuildmat.2017.03.009
30. Collepardi, M. *The new concrete*. Tintoretto. Rome, 2006. ISBN: 9788890146947
31. Topçu, İ. B., Uğurlu, A. Effect of the use of mineral filler on the properties of concrete. *Cement and Concrete Research*. 2003. 33. Pp. 1071–1075. DOI: 10.1016/S0008-8846(03)00015-2
32. Cepuritis, R., Mørtzell, E. Possibilities of improving crushed sand performance in fresh concrete by washing: a case study. *Materials and Structures*. 2016. 49(12). Pp. 5131–5146. DOI: 10.1617/s11527-016-0849-x
33. Bílý, P., Fládr, J., Chylík, R., Vráblík, L., Hrbek, V. The effect of cement replacement and homogenization procedure on concrete mechanical properties. *Magazine of Civil Engineering*. 2019. 86(2). Pp. 46–60. DOI: 10.18720/MCE.86.5
34. Hrbek, V., Prošek, Z., Chylík, R., Vráblík, L. The effect of micro-silica on the microscopic features of the UHPC composite and its inter-facial transition zone. *Acta Polytechnica CTU Proceedings*. 201. 15. Pp. 31–35. DOI: 10.14311/APP.2018.15.0031
35. Fládr, J., Bílý, P., Chylík, R., Prošek, Z.: Macroscopic and Microscopic Properties of High Performance Concrete with Partial Replacement of Cement by Fly Ash. *Solid State Phenomena*. 2018. 292. Pp. 108–113. DOI: 10.4028/www.scientific.net/SSP.292.108

36. Chylik, R., Šeps, K: Influence of cement replacement by admixture on mechanical properties of concrete. Proceedings of the 12th fib PhD Symposium in Civil Engineering. Czech Technical University. Prague, 2018. Pp. 1267–1274.
37. Oliver, W. C., Pharr, G. M. Measurement of hardness and elastic modulus by instrumented indentation: Advances in understanding and refinements to methodology. *Journal of Material Research*. 2004. 19. Pp. 3–20. DOI: 10.1557/jmr.2004.19.1.3
38. Constantinides, G., Chandran, K. R., Ulm, F.-J., Vliet, K.V. Grid indentation analysis of composite microstructure and mechanics: Principles and validation. *Material Science and Engineering A*. 2006. 430(1–2). Pp. 189–202. DOI: 10.1016/j.msea.2006.05.125
39. Scrivener, K.L., Patel, H.H., Pratt, P.L., Parrott, L.J. Analysis of phases in cement paste using backscattered electron images, methanol adsorption and thermogravimetric analysis. *MRS Proceedings 85*. Cambridge University Press. Cambridge, 1986. Pp. 321–332. DOI: 10.1557/proc-85-67
40. Nežerka, V., Trejbal, J.: Assessment of aggregate-bitumen coverage using entropy-based image segmentation. *Road Material and Pavement Design*. 2019. Pp. 1–12. DOI: 10.1080/14680629.2019.1605304
41. Kjellsen, K.O., Wallevik O.H., Fjällberg L. Microstructures and microchemistry of the paste-aggregate interfacial transition zone of high-performance concrete. *Advances in Cement Research*. 1998. 10(1). Pp. 33–40. DOI: 10.1680/adcr.1998.10.1.33
42. ČSN EN 206+A1 Concrete – Specification, performance, production and conformity. ÚNMZ. Prague, 2018.
43. ČSN EN 12390-3 Testing hardened concrete – Part 3: Compressive strength of test specimens. ÚNMZ. Prague, 2009.
44. ČSN ISO 1920-10 Testing of concrete – Part 10: Determination of static modulus of elasticity in compression. ÚNMZ. Prague, 2016.
45. Ambily, P. S., Umarani, C., Ravisankar, K. Studies on ultra high performance concrete incorporating copper slag as fine aggregate. *Construction and Building Materials*. 2015. 77. Pp. 233–240. DOI: 10.1016/j.conbuildmat.2014.12.092

Contacts:

Petr Bily, petr.bily@fsv.cvut.cz

Josef Fladr, fladr@fsv.cvut.cz

Roman Chylik, chylik@fsv.cvut.cz

Vladimir Hrbek, hrbek@fsv.cvut.cz

Lukas Vrablok, vrablok@fsv.cvut.cz

© Bily, P., Fladr, J., Chylik, R., Hrbek, V., Vrablok, L., 2020